ADEQUACY OF THERMOHYDRODYNAMIC MODEL OF THROUGH PENETRATION IN TIG AND A-TIG WELDING OF NIMONIC-75 NICKEL ALLOY*

D.V. KOVALENKO[1], **D.A. PAVLYAK**[2], **V.A. SUDNIK**[2] and **I.V. KOVALENKO**[1]
[1]E.O. Paton Electric Welding Institute, NASU, Kiev, Ukraine
[2]Tula State University, Tula, Russian Federation

Results of experiments on weld formation in TIG and A-TIG welding of Nimonic-75 alloy, and results of computer simulation of the effect of convection on «sand glass» shape of weld are presented. The experiments were carried out with and without activating flux PATIG Nim-75-A on 3.15 mm thick plates. Adequacy of the model was evaluated by comparing the sizes of the real and simulated weld sections. The causes of recirculation flows were analyzed. Correlation of the experimental and computation data was revealed.

Keywords: *TIG and A-TIG welding, nickel alloy, penetration, mathematical model, adequacy of mathematical model*

Positive results connected with an abrupt increase of penetration depth at activating flux deposition on the surface of metal to be welded in TIG welding (A-TIG process) of titanium obtained at the E.O. Paton Electric Welding Institute [1, 2] stimulated investigations on arc column contraction in TIG welding of steels and other materials [3–5].

Study [6] marked the beginning of investigations of convection in welding. This work is devoted to the influence of surfactants on penetration depth. Work [7] provides experimental proof of the postulates of [6] on the key factor in penetration depth, namely, change of the sigh of temperature coefficient of surface tension $d\sigma/dT$ from negative to positive sign. Addition of surfactants lowers surface tension at melting temperature, and values of $d\sigma/dT$ coefficient become positive. However, at temperature increase up to 1900 °C, surface tension reaches values characteristic for pure metal with a maximum at critical temperature, and values of $d\sigma/dT$ coefficient again become negative, as for pure metal.

World's first two-dimensional model of weld pool convection [8], created in 1983, provided theoretical confirmation of the postulates of [6] and showed that Marangoni surface tension forces are predominating, and together with the Lorentz electromagnetic forces they are responsible for appearance of double eddy regions. Later it was established [9] that the sign of thermal concentration dependence of surface tension and its values determine the direction of convective heat transfer under the arc and number of vortices. Simulation of the role of electromagnetic forces in A-TIG welding is carried on, and the nature of the mechanism of this phenomenon still has not been determined. It is established that arc contraction does not affect austenitic steel penetration, but it should be taken into account as an auxiliary factor [10, 11]. It was proved here that electromagnetic convection promotes deep penetration [12] and the centrifugal component of the electromagnetic force is the dominating factor of penetration [13]. Published results are given only for the simplest axisymmetrical case of a stationary heat source of incomplete penetration on a stationary item from austenitic steel.

Technology of A-TIG welding of Nimonic-75 nickel alloy was tried out for the first time at PWI [14]. It is based on application of a short (1.5 mm) arc and activating salt-oxide flux PATIG Nim-75-A, containing metal fluorides and oxides. Fluorides promote arc contraction [5] and influence development of physical processes in it [15, 16]. Fluoride fluxes allow welding titanium sheets of up to 8 mm thickness [17, 18]. A team of scientists led by B.E. Paton [19] developed a theoretical model of arc contraction by fluoride fluxes. For sodium fluoride NaF at welding current I_w = 100 A value of anode spot radius $r_a \approx 1.5$ mm was obtained.

Another nickel alloy Nimonic-263 was welded over a layer of isolated titanium oxides and their mixtures, and the welding process was simulated using PHOENICS program [20]. Calculation results differed from experimental data.

Computer simulation has recently become the main method of scientific investigations. Program code developers and experimenters using such programs, face the following question: how the error of simulation results should be assessed? Computer simulation ends by prediction of the result of welding, and the most important characteristic of the prediction is the confidence level. According to [2] prediction error is a

*Published by the materials of a paper presented at the V International Conference on Mathematical Simulation and Information Technologies in Welding and Related Technologies (May 25–28, 2010, Katsively vil., Crimea, Ukraine).

vector sum of errors of simulation and experiment, allowing for the normal random distribution of data. The significance of the discrepancy between the results of simulation (prediction) and experimental data is determined by statistical criteria, for instance in comparison of dispersions by Fisher criterion [21], or at unknown dispersion (often the case in practice) by Student criterion [22].

The purpose of this work is comparison of experimental shape of the through-penetration weld made on Nimonic-75 alloy by TIG and A-TIG welding with the simulated shape, as well as analysis of the influence of melt convection on weld shape.

Experimental studies. These were conducted by automatic gravity welding of butt joints of plates from Nimonic-75 nickel alloy 3.15 mm thick and of 200 × × 20 mm size. Composition of the studied alloy according to [23] is as follows, wt.%: 0.14 C; 0.14 Si; 0.39 Mn; 21.Cr; 3.4 Fe; 0.28 Ti; 0.05 Cu; 0.001 S; 0.008 P; 0.0175 O; Ni being the base.

Nonconsumable tungsten electrode with 2 wt.% Th of 2.1 mm diameter with sharpening angle of 30° and blunting of 0.5–0.8 mm was used. Argon with not more than 0.1 wt.% of impurities was used as shielding gas (10 l/min flow rate), as well as for weld root shielding (2 l/min flow rate). Welding was performed with VSVU-315 welding power source. Experiments were conducted with application of aerosol activating flux (activator) PATIG Nim-75-A and without it at current I_w = 40–240 A, arc length was 1–4 mm, welding speed was v_w = 50–500 mm/min.

In each experiment a uniform layer of activator 80–100 μm thick was applied on the plate surface. During experiments welding current, arc voltage and welding speed were monitored. After welding, macrosections were prepared and measurements of geometrical dimensions of welds and visual assessment of their formation quality were performed.

Figure 1 shows cross-sections of through-penetration welds made on Nimonic-75 alloy at the same (200 mm/min) welding speed at I_w = 100 A (A-TIG welding) and 180 A (TIG welding). As is seen from the Figure, in A-TIG welding process, welding current and heat input can be reduced almost 2 times to achieve through penetration of the weld, compared to TIG welding.

Figure 2 presents macrosections of a weld made by A-TIG welding, which were cut out of different locations on a sample of Nimonic-75 alloy along its length — at the start (Figure 2, *a*), in the middle

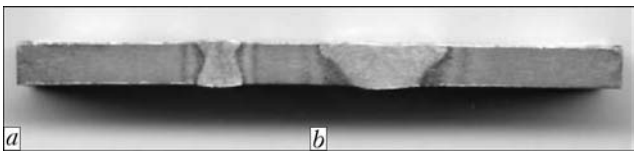

Figure 1. Transverse macrosections of through-penetration welds made on Nimonic-75 alloy by A-TIG welding at I_w = 100 A (*a*) and TIG welding at I_w = 180 A (*b*) at the same (200 mm/min) welding speed

(Figure 2, *b*) and at the end (Figure 2, *c*) (I_w = 100 A, arc voltage U_a = 10 V, arc length of 1.5 mm, v_w = = 200 mm/min). The Figure clearly shows the scatter of weld shape and dimensions across its width, which is caused by certain instability of weld formation in through-penetration gravity welding.

Simulation of welding processes. Thermohydrodynamic model of though penetration, developed in Tula State University, is based on equations of energy, Navier–Stokes and continuity with the respective boundary conditions allowing for the features of TIG and A-TIG welding. It is used for simulation of the considered processes.

Thremophysical properties of Nimonic-75 alloy are studied only at room temperature [23]. An analog of the above alloy in Russia is KhN55VMTKYu nickel alloy, in the USA — Inconel-718 [24], in Germany — Nicrofer 2520-alloy 75 [25]. Temperature dependencies of thermophysical properties of Inconel-718 and Nicrofer 2520-alloy 75 are known from [24, 25], their comparison with reference points of Nimonic-75 alloy shows good correlation.

For TIG welding process the following initial mode parameters were assumed: I_w = 180 A, U_a = 9 V, arc length of 1.5 mm, short arc efficiency of 94 %, v_w = 200 mm/min, temperature coefficient of surface tension of −0.017 N/(cm·K) [24], radii of electric and thermal spots of 5.1 and 6.8 mm, respectively.

Calculated maximum temperature of the weld pool was T_{max} = 1780 °C, calculated weld width — 8.87 mm, experimental value — 10.5 mm, calculated penetration width — 5 mm, experimental value — 0–5 mm. Instability of penetration width in the experiment is attributable to selection of the mode in the region of transition from incomplete (I_w = 170 A) to through (I_w = 180 A) penetration (Figure 3). Assessment of the position of penetration boundary can be determined by the assumed melting temperature of the alloy (liquidus temperature T_l = 1380 °C) or coherence (continuity) temperature T_c, at which the liquid phase is absent at boiling temperature of 1367 °C equal to $T_l - (T_l - T_s)/3$, where T_s is the

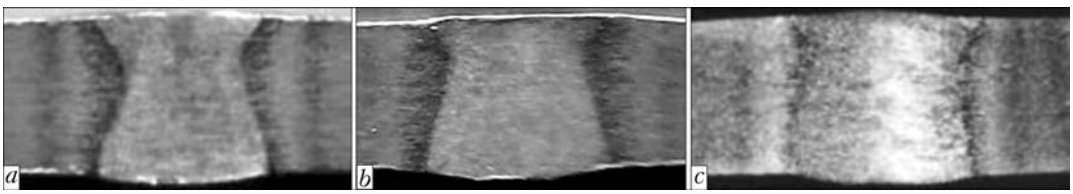

Figure 2. Transverse macrosections of a weld made on Nimonic-75 alloy by A-TIG welding (for *a–c* see the text)

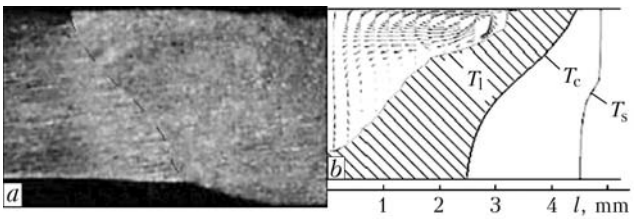

Figure 3. Experimental (*a*) and calculated (*b*) section of welds made by TIG welding at I_w = 180 A

solidus temperature [26]. In Figure 3, *b* this region is hatched.

For A-TIG welding process the following initial parameters of the mode were assumed: I_w = 100 A, U_a = 10 V, arc length of 1.5 mm, short-arc efficiency of 94 %, v_w = 200 mm/min. Allowing for the features of this process the following was assumed: heat spot radius of 2.2 mm (because of insulating action of activating flux); current spot radius of 0.9 mm (because of arc contraction by fluorine); on the upper surface temperature coefficient of surface tension of +0.01 N/(cm·K) allowing for reverse Marangoni convection; on the lower surface where the conditions were unchanged, temperature coefficient of surface tension was equal to –0.017 N/(cm·K).

Figure 4 shows a three-dimensional view of a plate from Nimonic-75 alloy at simulation of the process of A-TIG welding with non-characteristic for arc welding width and shape of the weld. Maximum weld pool temperature T_{max} = 2700 °C is in good agreement with the current concepts of nonconsumable electrode welding, allowing for the cooling action of the evaporation process, which was taken into account in the model boundary conditions.

Figure 5 gives the results of calculation of weld longitudinal section, made by A-TIG welding (x = = –12 mm), which are indicative of good reproducibility of weld shape in the form of «sand glass». Analysis of the obtained results shows that two eddy regions with Marangoni convection form in a weld pool with two free surfaces. At the lower surface of the weld pool temperature-capillary Marangoni flow has a classical shape — from weld pool center to its edges. Now, on the upper surface the flow pattern is more complicated with elements of both straight (from center to edges of weld pool) and reverse Marangoni convection towards weld pool center. Cross-sectional dimensions of the weld in the form of «sand glass» and their flow patterns are different in different sections. For such patterns three-dimensional volume presentation of the flows is more rational, similar to how it is presented in [26].

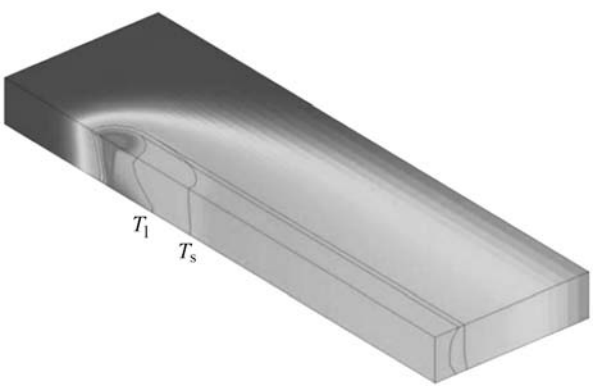

Figure 4. Three-dimensional view of a plate from Nimonic-75 alloy at simulation of A-TIG process

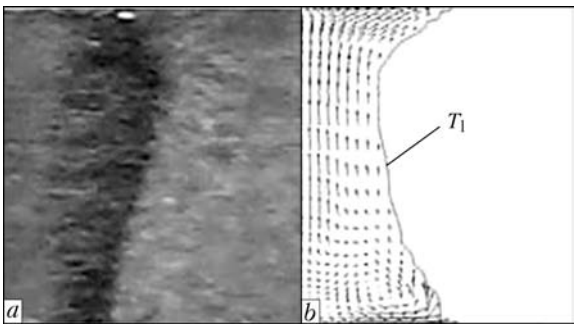

Figure 5. Experimental (*a*) and calculated (*b*) section of welds made by A-TIG welding at I_w = 100 A (arrows indicate the direction of liquid metal motion at maximum speed of 0.232 m/s)

Proposed possible mechanism of through penetration in A-TIG welding consists in formation of the following flows of weld pool liquid metal: main flow of heat transfer of over-heated melt across the sheet thickness in the contracted arc zone caused by magnetic forces and determining the width of the weld narrow neck in the form of «sand glass» and two additional fluxes of recirculation boundary flows caused by thermocapillary forces on both the weld pool surfaces, which determine the width of the weld molten zones decreasing to the neck size.

Adequacy of mathematical model. This term usually means the degree of correspondence of the same properties of the object and the model. Procedure of assessment of adequacy of computer simulation of the process of A-TIG welding of Nimonic-75 alloy characterized by penetration in the form of «sand glass» (see Figure 5), and TIG welding consisted in statistical processing of experimental results and obtaining an evaluation of mean-root-square deviation S of parameter values (each of weld width dimensions on upper W and lower B sides of the sheet, as well as width W_n and height H_n of «sand glass» neck):

$$S = \sqrt{\frac{1}{n-1}\sum_{j=1}^{n}(y_{exp} - y_{cal})^2},$$

where n is the sample size; y_{exp} and y_{cal} are the experimental and calculated values of the parameter.

Adequacy assessment was performed by Student's statistical criterion

$$t_{m,\,1-\alpha} \geq \frac{y_{exp} - y_{cal}}{S}\sqrt{n},$$

where $t_{m,\,1-\alpha}$ is the tabulated value of t-distribution; α is the level of significance equal to 0.05.

Results of experiments and calculations are given in Tables 1 and 2.

Table 1. Results of experiments and calculations obtained across the width of welds made by A-TIG and TIG on plate upper W and lower B surfaces

Welding process	I_w, A	v_w, mm/min	Weld width, mm					
			W_{exp}	W_{cal}	S	B_{exp}	B_{cal}	S
A-TIG	100	200	3.9	3.60	0.72	3.6	3.1	0.42
			3.8			4.1		
			3.3			3.4		
			Average 3.67			Average 3.7		
TIG	180	200	10.5	8.87	1.62	5.0	2.5	2.95
			10.0			4.6		
			9.0			3.6		
			Average 9.83			Average 4.4		

Notes. 1. Here and in Table 2 Student's criterion $t_{m,\,1-\alpha} = 4.3$. 2. Condition of adequacy is assumed. 3. Indices «exp» and «cal» indicate experimental and model values, respectively.

Suggested hypotheses of coincidence of average values of two sets — experimental and calculates ones, assessed by Student's criterion, are accepted with confidence probability of 0.95.

Thus, experiments on A-TIG welding of plates from Nimonic-75 nickel alloy 3.15 mm thick showed that at complete (through) penetration the weld takes the shape of «sand glass». Simulation by a thermohydrodynamic model of weld pool in A-TIG welding of plates of Nimonic-75 nickel alloy reproduces the shape of complete (through) penetration in the form of «sand glass». Assessment of the accuracy of reproducing cross-sectional dimensions of weld by this model by comparing average experimental and calculated values from Student's criterion showed the adequacy of this model with confidence probability of 0.95. Proposed mechanism of through penetration of A-TIG welding includes the main flow of heat transfer of overheated melt across sheet thickness in the contracted arc zone caused by electromagnetic forces and determining the width of the narrow neck in the form of «sand glass», as well as two additional recirculation boundary flows caused by thermocapillary forces on both surfaces of the weld pool and determining the width of the weld molten zones which are reduced to the size of «sand glass» neck.

Table 2. Results of experiments and calculations obtained by width W_n and height H_n of weld neck in the form of «sand glass» at simulation of A-TIG welding process

I_w, A	v_w, mm/min	Neck width, mm			Neck height, mm		
		$W_{n\,exp}$	$W_{n\,cal}$	S	$H_{n\,exp}$	$H_{n\,cal}$	S
100	200	3.1	0.95	1.32	1.5	0.8	0.28
		3.0			1.2		
		2.4			0.9		
		Average 2.83			Average 1.2		

1. Gurevich, S.M., Zamkov, V.N., Kushnirenko, N.A. (1965) Increase in effective penetration during argonarc welding. *Avtomatich. Svarka*, **9**, 1–4.
2. Gurevich, S.M., Zamkov, V.N. (1966) Some peculiarities of nonconsumable electrode welding of titanium with application of fluxes. *Ibid.*, **12**, 12–16.
3. Ostrovsky, O.E., Kryukovsky, V.N., Buk, B.B. et al. (1977) Effect of activating fluxes on penetrating capacity of welding arc and energy concentration in anode spot. *Svarochn. Proizvodstvo*, **3**, 3–4.
4. Savitsky, M.M., Leskov, G.I. (1980) Mechanism of effect of electronegative elements on penetrating capacity of arc with tungsten cathode. *Avtomatich. Svarka*, **9**, 17–22.
5. Zamkov, V.N., Prilutsky, V.P. (1987) Distribution of current density in anode spot during welding of titanium. *Ibid.*, **3**, 19–22.
6. Heiple, C.R., Roper, J.R. (1982) Mechanisms for minor element effects on GTA fusion zone geometry. *Welding J.*, 61(**4**), 97–102.
7. Mills, K.S., Keene, B.I., Brooks, R.F. et al. (1984) The surface tension of 304 and 316 type steels and their effects on weld penetration. In: *Proc. of Conf. on Centenary of Metallurgy Teaching* (Glasgow, 1984), 1–11.
8. Oreper, G.M., Eagar, T.W., Szekely, J. (1983) Convection in arc weld pools. *Welding J.*, 62(**11**), 307–312.
9. Zhao, Y. (2006) The study of surface-active element oxygen on flow patterns and penetration in A-TIG welding. *Metallurg. and Mater. Transact. B*, 37(**6**), 485–493.
10. Tanaka, M. (2005) Effect of surface active elements on weld pool formation using TIG arcs. *Welding Int.*, 19 (**11**), 870–876.
11. Zhang, R.H., Fan, D. (2007) Numerical simulation of effects of activating flux on flow patterns and weld penetration in A-TIG welding. *Sci. and Techn. of Welding and Joining*, 12(**1**), 15–23.
12. Wang, Y., Shi, O., Tsai, H.L. (2001) Modelling of the effects of surface-active elements on flow patterns and weld pool penetration. *Metalurg. and Mater. Transact. B*, 32(**2**), 145–161.
13. Yushchenko, K.A., Kovalenko, D.V., Krivtsun, I.V. et al. (2008) Experimental studies and mathematical modelling of metal penetration in TIG and A-TIG stationary arc welding. *IIW Doc. 212-1117–2008*.
14. Yushchenko, K.A., Kovalenko, I.V., Kovalenko, D.V. et al. (2000) A-TIG welding of nickel alloy Nimonic-75. *Svarshchik*, **4**, 26–27.
15. Lucas, W., Howse, D. (1996) Activating flux — increasing the performance and productivity of the TIG and plasma processes. *Welding & Metal Fabrication*, 65(**1**), 11–17.
16. Howse, D., Lucas, W. (2000) Investigation into arc constriction by active fluxes for tungsten inert gas welding. *Sci. and Techn. of Welding and Joining*, 5(**3**), 189–193.
17. Perry, N., Marya, S., Soutif, E. (1999) *New perspectives of flux assisted GTA welding in titanium structures*, 55–62.

18. Leconte, S., Pillard, P., Chaelle, P. et al. (2007) Effect of flux containing fluorides on TIG welding process. *Welding and Joining*, 12(**2**), 120–126.
19. Paton, B.E., Zamkov, V.N., Prilutsky, V.P. et al. (2000) Contraction of the welding arc caused by flux in tungsten-electrode argonarc welding. *The Paton Welding J.*, **1**, 5–11.
20. Xu, Y.L., Dong, Z.B., Wei, Y.H. et al. (2007) Marangoni convection and weld pool shape variation in A-TIG welding process. *Theoretical and Applied Fracture Mechanics*, **48**, 178–186.
21. Sudnik, W., Radaj, D., Erofeev, W. (1998) Validation of computerized simulation of welding processes. In: *Mathematical modelling of weld phenomena 4*. London: IOM Commun., 477–493.
22. Erofeev, V.A., Karpukhin, E.V., Sudnik, V.A. (2001) Computer simulation of nonstationary laser welding. Computer technologies in joining of materials. In: *Proc. of 3rd All-Union Sci.-Techn. Conf.* (Tula, 9–11 October 2001). Tula: TulGU, 111–118.
23. *B5 HR 20–72*: Specification for nickel-chromium-titanium heat-resisting alloy plate, sheet and strip. Great Britain.
24. Sudnik, V.A., Erofeev, V.A., Richter, K.H. et al. (2006) Numerical modelling of the EBW process. In: *Computer techn. in welding and manufacturing*. Kiev: PWI, 295–300.
25. *Nicrofer 2520-alloy 75*: ThissenKrupp VDM Material Data Sheet, 4035.
26. Zhao, C.X., Van Steijn, V., Richardson, L.M. et al. (2007) Unsteady interfacial phenomena during inward weld pool flow with an active surface oxide. *Sci. and Techn. of Welding and Joining*, 14(**2**), 132–140.

OPTIMAL REDUCTION OF WORKING PRESSURE IN PIPELINES FOR WELDING REPAIR OF THINNING REGIONS

V.I. MAKHNENKO, V.S. BUT, S.S. KOZLITINA, L.I. DZYUBAK and **O.I. OLEJNIK**
E.O. Paton Electric Welding Institute, NASU, Kiev, Ukraine

The possibility of using welding to repair defects of corrosion origin in walls of pressurised pipelines is considered. It is shown that the safety of welding operations is affected not only by the overall size of a defect, but also by the shape of a pipe wall thinning. Calculation algorithms are applied to substantiate the possibility of repair of defects by overlaying welding due to optimal reduction of internal pressure in the main line for a period of repair.

Keywords: *main pipeline, welding repair, overlaying welding, sizes of defects, residual thickness of pipe wall, optimal pressure*

Repair of main pipelines by welding without interruption of their operation, i.e. in a pressurised state, is finding now an increasingly wider application, as it allows an optimal reduction of downtime and pollution of the environment. A key point of this technology is safety of repair operations performed on a pressurised pipeline depending on the type of a defect, its shape and size. The most frequent defects in underground main gas pipelines are wall thinning defects of the corrosion origin, which are associated with violation of waterproof insulation. Such defects with overall sizes $s_0 \times c_0 \times a$ (Figure 1), where s is the size of a defect along the pipe axis, and c and a are the sizes of the defect on the circumference and through the wall thickness, respectively, are well studied. Different criteria are available for estimation of the risk of fracture within the zones of such defects depending on their sizes, geometric parameters of a pipeline, its mechanical properties, pressure inside a pipe [1–3], etc. For example, study [1] gives fairly simple relationships based on numerous experimental investigations, which make it possible to judge whether the wall thinning defects in pipelines are permissible or not depending on the above parameters.

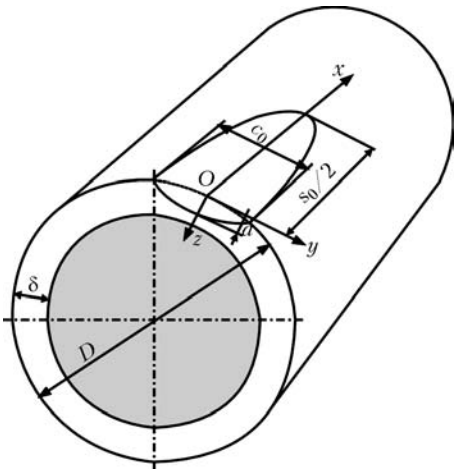

Figure 1. Schematic of pipeline with thinning defect in the form of an ellipsoid measuring $s_0 \times c_0 \times a$ before welding

The condition of permissibility of a corrosion thinning defect with sizes $s(t)$ and $c(t)$ at time moment t in a pipeline, according to [3], can be written down as

$$y(t) = \delta - a(t) - [\delta]R_j > 0, \quad (1)$$

where

$$R_j = \delta_{\min}/[\delta] \quad (j = s, c); \quad (1a)$$

$\delta_{\min}$ is the minimal measured wall thickness within the defect zone ($\delta_{\min} = \delta - a$); and $[\delta]$ is the permissible calculated thickness of the pipeline wall without considering the thinning defects, i.e.

$$[\delta] = \frac{PD}{2[\sigma]}, \quad (2)$$